Bayesian operational modal analysis of closely spaced modes for monitoring wind turbines

Clemens Jonscher*, Sören Möller, Leon Liesecke, Benedikt Hofmeister, Tanja Grießmann, Raimund Rolfes

Institute of Structural Analysis, Leibniz Universität Hannover, Appelstraße 9A, 30167 Hannover, Germany

---

Abstract

In this study, the applicability of Bayesian operational modal analysis (BAYOMA) to an operating onshore concrete-steel hybrid wind turbine tower is investigated. The results of the identification then provide reliable parameters for the structural health monitoring (SHM) of the tower.

In the context of wind turbines, typical assumptions of linear time-invariant OMA methods are violated, so the validity of the identification uncertainties of BAYOMA is not necessarily given. In addition, closely spaced modes occur, for which the mode shape in particular is subject to high uncertainty. It can be stated, that the main part of the mode shape uncertainty corresponds to the alignment of these in the mode subspace.

Due of these challenges, mode shapes are generally not taken into account when monitoring wind turbine towers. In order to include the mode shape in SHM scheme, the second-order modal assurance criterion (S2MAC) is applied in this study. This metric is able to eliminate the alignment uncertainty by comparing the mode shape with a mode subspace.

Besides mode shapes, the reliability of natural frequencies and damping can also be better quantified by knowing the identification uncertainty. This finally enables a well-founded selection of suitable monitoring parameters for the future application of SHM for wind turbines.

Keywords: `BAYOMA`, `wind turbine tower`, `structural health monitoring`, `uncertainty quantification`, `closely spaced modes`

1. Introduction

Wind energy already accounts for the largest share of renewable electricity generation in the European Union (EU). In 2018, wind energy accounted for 18.4% of the electricity generation capacity in the EU, with an installed capacity of 170 Gigawatt (GW) onshore and 19 GW offshore [1]. As in many engineering disciplines, efficient operation and maintenance also play a major role in the field of wind turbines. Consequently, there is a great motivation to implement effective monitoring strategies in order to reduce maintenance costs and increase safety at the same time [2]. In the field of civil engineering, the associated monitoring concept is referred to as *Structural Health Monitoring* (SHM). In this context, a distinction is generally made between model-based SHM and data-based SHM. Data-based SHM is currently considered the predominant approach [3]. To apply data-based methods, a suitable measurement concept is crucial. A global monitoring approach is often used due to a more

*Corresponding author
Email address: `c.jonscher@isd.uni-hannover.de` (Clemens Jonscher)

economic measurement concept compared to local approaches. Here, a small number of sensors is used to determine information about the condition of the whole structure in terms of structural dynamics. Based on the measured system response data, monitoring parameters (MP) are extracted using feature extraction techniques. From these parameters, a subset of parameters is determined that can distinguish between a damaged and an undamaged state of the structure [4]. In this context, operational modal analysis (OMA) methods are commonly used to identify modal parameters as MPs. Typically, the result of the identification of modal parameters includes natural frequencies, damping and mode shapes and does not require measurements of the excitation forces. In the recent years, OMA methods, like *Bayesian Operational Modal Analysis* (BAYOMA) [5], were developed to not only identify the modal parameters but also their uncertainties.

Various OMA methods have been successfully used in recent years for monitoring the supppot structures of wind turbines. In particular, the covariance-based *Stochastic Subspace Identification* (SSI) [6, 7, 8], the *poly-reference Least Squares Complex Frequency* (pLSCF) [7, 8] and the *Frequency Domain Decomposition* (FDD) [9, 10] are to be mentioned here. The aim of this work is to investigate the suitability of the relatively recent method BAYOMA for monitoring of an existing hybrid tower of an onshore wind turbine. Challenges in this specific application include the identification of closely spaced modes, harmonic excitation, a short evaluation time relative to the oscillation period, high damping, and non-stationarity due to environmental and operational conditions

(EOC).

The low-frequency system dynamics are challenging, because the measurement chain must be designed and calibrated for the low-frequency range [11]. In addition, this makes the identification of the modal parameters much more uncertain [12]. The Identification of a wind turbine tower is further complicated by the fact that the damping of the fore-aft mode (FA) at higher rotor speeds is greater than that of the side-to-side mode (SS) [9]. If the evaluation time is extended beyond the commonly used 10 minutes to improve the identification accuracy, there is a risk that the identification will become less reliable due to the instationarities caused by varying EOCs. This problem can be solved using time-varying systems, like time-varying autoregressive moving average models (TV ARMA) [13]. However, linear OMA methods are commonly used for vibration-based monitoring, which assume a time-invariant system under white noise excitation. These identification procedures were found to be robust even when the assumption of time invariance was violated, as found by Brownjohn et al. [14], who applied BAYOMA to offshore lighthouses. Another challenge is the harmonic excitation, which can lead to distortion of the natural frequencies [6]. Possible approaches in the context of monitoring wind turbine towers for example do not consider the identified natural frequencies in the range of higher harmonics of the rotor [15], or use cluster analysis to separate natural frequencies from harmonics [16].

In tower structures, it is common to deal with closely spaced modes which are challenging to identify, especially regarding the mode shapes. Au et al. [12]

show that the largest uncertainty in the case of closely spaced modes occurs for the identification of the mode shapes. This uncertainty can be divided into two parts. The first part is the uncertainty of the mode subspace (MSS) spanned by the dominant vibration shapes. This uncertainty is similar to the uncertainty of mode shapes in the well-separated case, which depends mainly on the noise of the measurement chain. Hence, in case of low-noise data, the MSS can be identified very reliably. The second part of the uncertainty of the mode shape is the alignment of the mode in the MSS. The uncertainty of the alignment identification increases significantly with the increase in closeness of the frequencies [17]. Therefore, an extension of the well-known modal assurance criterion (MAC) in form of the subspace of order 2 MAC (S2MAC) [18] was developed, which compares a mode shape with a subspace. This metric can provide in case of closely spaced modes less uncertain results than the classical MAC, because it eliminates uncertainty in the alignment. This allows detection of system changes for symmetrical tower structures based on mode shapes [19, 17].

In this study, BAYOMA is used as it identifies their uncertainties in addition to the modal parameters, and gives good results in the context of closely spaced bending modes of tower structures [14, 17]. The aim of this study is to investigate the applicability of BAYOMA with the associated identification uncertainties on a hybrid tower of an onshore wind turbine under operating conditions in order to obtain meaningful monitoring parameters for structural health monitoring. The structure of the work is as follows: Section 2 introduces the theory used in the following chapters. Section 3 describes the wind turbine tower under investigation and its dynamics are analysed in more detail, taking the identification uncertainty into account. Finally, in Section 4, the study is summarised and an outlook is given.

2. Theory

This section explains shortly BAYOMA and the metrics for comparing mode shapes of closely spaced modes. In addition, the mode tracking of the modes of a wind turbine tower under operation is presented.

2.1. Bayesian operational modal analysis

In this study, the natural frequencies and mode shapes are identified with the frequency domain method BAYOMA [5, 20]. The basis of BAYOMA is the discrete Fourier transform (DFT) of a Gaussian distributed signal. Assuming a long measurement time and a high sampling rate, a DFT of the individual frequency base point is statistically independent of all other base points and also Gaussian distributed [21]. By assuming an equally distributed prior of the modal parameters, the likelihood becomes proportional to the posterior.

The likelihood of the DFT is therefore a multivariate Gaussian distribution. The related covariance matrix is the excpected power spectral density matrix of m dominating modes. In case of several closely spaced modes in a considered frequency range, the variables to be identified increase significantly due to the number of mode shapes. To reduce numerical complexity, the mode subspace

(MSS) is first identified and then the alignment of the modes in the subspace as well as the associated natural frequencies and damping are identified. The MSS, noted as $\boldsymbol{\Psi}$, is a subspace spanned by the m dominating vibration shapes in the considered frequency range. Assuming real mode shapes, these are formed from the m largest eigenvectors of the summed real spectral matrix in the considered frequency range. Instead of the entire mode shape, the identification only needs to determine the angles $\boldsymbol{\beta}$ of the transformation matrix $\boldsymbol{T}$ corresponding to the orientation of the mode within the mode subspace. For $m = 2$, this can be defined as

$$\boldsymbol{\Phi} = \boldsymbol{\Psi}_{1,2}\boldsymbol{T}(\beta_1, \beta_2) = \boldsymbol{\Psi}_{1,2} \begin{bmatrix} \cos(\beta_1) & \cos(\beta_2) \\ \sin(\beta_1) & \sin(\beta_2) \end{bmatrix}. \tag{1}$$

This provides the expected value $\mathbb{E}$ of the theoretical power spectral density matrix of two dominating modes

$$\mathbb{E}_k(\boldsymbol{\Theta}) = \boldsymbol{\Psi}_{1,2}\boldsymbol{T}\boldsymbol{H}_k(\boldsymbol{\Psi}_{1,2}\boldsymbol{T})^T + S_e\boldsymbol{\Psi}\boldsymbol{\Psi}^T, \tag{2}$$

where $\mathbf{H}_k$ is a diagonal matrix containing the two theoretical power spectral densities of equivalent one-mass oscillators for the frequency support point k. The optimisation parameters $\boldsymbol{\Theta}$ are the natural frequencies, modal damping, modal force, the angles of the transformation matrix as well as the model error S_e. The identification of the most probable values of $\boldsymbol{\Theta}$ for a specified frequency range is preformed by minimising the negative log likelihood function $L(\mathbf{\Theta})$

$$L(\mathbf{\Theta}) = n_c N_f \ln\pi + \sum_{k=1}^{N_f} \ln\left|\mathbb{E}_k(\mathbf{\Theta})\right| + \sum_{k=1}^{N_f} \mathcal{F}_k^* \mathbb{E}_k(\mathbf{\Theta})^{-1} \mathcal{F}_k, \tag{3}$$

where N_f is the number of considered frequency points and $\mathcal{F}$ is the DFT of the measured signal. The covariance matrix of the Gaussian approximation of the posterior distribution is calculated with the inverse Hessian matrix of the negative log likelihood function at the most probable values. In a subsequent step, the MSS can be adjusted using a Newton iteration [20].

2.2. Metrics for mode shapes

For almost rotationally symmetric tower structures, closely spaced modes occur for the bending modes. For such structures, previous investigations have shown that the mode shapes have much higher associated identification uncertainty than in the case of well-separated modes [12, 19]. Most of the uncertainty is in the alignment of the mode shape in the MSS, so the widely used Modal Assurance Criterion (MAC) [22] to compare two mode shapes $\boldsymbol{\varphi}_j$ and $\boldsymbol{\varphi}_k$, defined as

$$\mathrm{MAC}_{j,k} = \frac{|\boldsymbol{\varphi}_j^H \boldsymbol{\varphi}_k|^2}{\boldsymbol{\varphi}_j^H \boldsymbol{\varphi}_j \boldsymbol{\varphi}_k^H \boldsymbol{\varphi}_k}, \tag{4}$$

becomes very uncertain as well. This is visualised by the identification uncertainty of an exemplary closely spaced mode shape using a Monte Carlo simulation in Figure 1A, where the scatter is evident. Moreover, no Gaussian distribution can be assumed when the MAC values approach one. The assump-

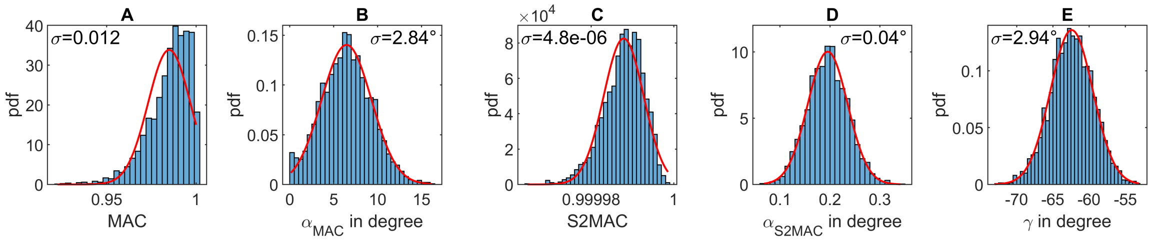

Figure 1: Histograms with normal distribution fits and the standard deviation σ of the MAC, α_{MAC}, S2MAC, α_{S2MAC} and the directional angle γ of one exemplary mode shape of a closely spaced bending mode pair, normalised according to the probability density functions (pdf). The determination is performed using the covariance matrix of the mode shape and the Monte Carlo method with 3000 samples.

tion of a beta distribution is better suited to modelling the MAC distribution [17].

To eliminate the alignment uncertainty, the subspace of order 2 Modal Assurance Criterion (S2MAC) was developed [18]. The S2MAC calculates the best MAC between the mode shape φ_i and the MSS spanned by two vibration shapes vectors $\boldsymbol{\psi}_j$ and $\boldsymbol{\psi}_k$. In the case of normalised real mode shapes of length one, the S2MAC is defined as

$$\mathrm{S2MAC}_{i,jk} = \frac{(\boldsymbol{\varphi}_i^T \boldsymbol{\psi}_j)^2 - 2(\boldsymbol{\varphi}_i^T \boldsymbol{\psi}_j)(\boldsymbol{\psi}_j^T \boldsymbol{\psi}_k)(\boldsymbol{\varphi}_i^T \boldsymbol{\psi}_k) + (\boldsymbol{\varphi}_i^T \boldsymbol{\psi}_k)^2}{1 - (\boldsymbol{\psi}_j^T \boldsymbol{\psi}_k)^2}. \tag{5}$$

Figure 1C shows that the scattering is significantly reduced compared to the regular MAC and the distribution is closer to a Gaussian distribution. However, a slight skewness of the distribution is still present. The MAC and S2MAC are relatively insensitive to small changes of the mode shape relative to the reference shapes. Since both metrics represents a squared scalar product of vectors normalised to one, the angles α_{MAC} and α_{S2MAC} can be derived

$$\alpha_{\mathrm{MAC}} = \arccos(\sqrt{\mathrm{MAC}}). \tag{6}$$

The angle of the MAC is simply the angle between the two mode shapes, for the S2MAC it is the smallest angle between the mode shape and the MSS. Due to this transformation, α_{MAC} and α_{S2MAC} become Gaussian distributed, which is shown in Figure 1B and 1D. In Figure 1B, the α_{MAC} illustrates that the angle representation can contain a deviation from the Gaussian distribution close to zero, due to the fact that the angles are constrained to be larger than 0. This error occurs in the case of large uncertainty and mean values close to 0. In the context of wind turbines, this can occur especially with the significantly less reliable α_{MAC}.

The alignment uncertainty can be approximated by the directional angle γ in the case of a tower structure and a same sensor setup at all measurement levels in both spatial directions analogous to the calculation of the mean phase [23], as shown in [17]

$$\gamma = \arctan\left(\frac{-V_{12}}{V_{22}}\right) \text{ with } \boldsymbol{USV}^T = [\boldsymbol{\varphi}_x \ \boldsymbol{\varphi}_y], \tag{7}$$

where $\boldsymbol{USV}^T$ is the singular value decomposition, $\boldsymbol{\varphi}_x$ are the entries of the mode shape in x-direction, and $\boldsymbol{\varphi}_y$ are the entries of the mode shape in y-direction. V_{12} and V_{22} are the corresponding elements of the matrix $\boldsymbol{V}$. The distribution of the direction angle in Figure 1E demonstrates clearly that it can be assumed as Gaussian. It is remarkable that the standard deviation of the α_{MAC} and the direction angle are quite similar. This is an indication that the alignment uncertainty of the mode in the MSS is well described by the directional angle γ in the case of bending modes of tower structures. In this study, the uncertainties of the mode shape metrics are determined with a 3000 sample Monte Carlo simulation, which takes into account the covariance matrix of the mode shape identification. The distribution of the mode shape metrics α_{MAC} , α_{S2MAC} and γ assumed to be Gaussian despite the possible small error.

2.3. Mode tracking of closely spaced modes

In the case of changing modal parameters caused by varying EOCs or mechanical changes, mode tracking becomes a challenge. Here, the identified natural frequencies and mode shapes are compared with reference frequencies or reference shapes. As demonstrated in the previous chapter, an assignment of the mode shapes in the presence of closely spaced modes is associated with great uncertainties. In case of support structures of wind turbines, this is further complicated, because the mode alignment changes along with a changing nacelle positions. A typical approach for this application is to rotate the reference mode shape depending on the nacelle position [16]. Subsequently, the rotated reference mode shape can be compared to the identified mode with the MAC, such that it becomes insensitive to the nacelle angle. For this study, a similar procedure was used, which is shown in Figure 2. First, the modal parameters and the associated uncertainties are identified from the acceleration measurement data using BAYOMA. Since BAYOMA is a non-parametric identification

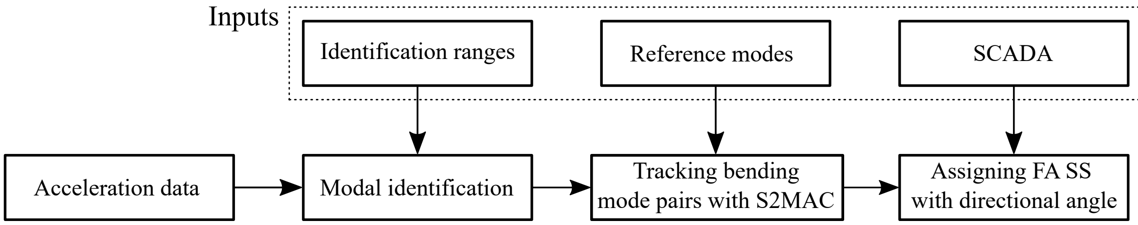

Figure 2: Sequence of identification and mode tracking used to monitor the support structure of a wind turbine.

method, the identification ranges and the number of modes within a frequency range are required as prerequisite information. These informations can be provided either automatically, according to Brincker et al. [24] or manually. In this work, the identification ranges are set manually. This has the advantage that only the modes of interest are identified. However, care must be taken to ensure that these ranges are sufficiently large to include the full range of variability and that a verification of the identification results is carried out. To verify that two different modes have been identified, it is required that the maximum MAC of the two closely spaced mode shapes does not exceed 0.5 to obtain two different modes and that the identified natural frequencies are within the identification range.

In a further part of the verification, the S2MAC is used to check whether the identified mode matches the previously determined reference MSS. This has the advantage that the alignment of the mode shape in the mode subspace, which is the main uncertainty of the mode shape for closely spaced modes, does not influence the bending mode pair tracking process. In addition, the influence of the nacelle position on the bending mode pair tracking can be eliminated,

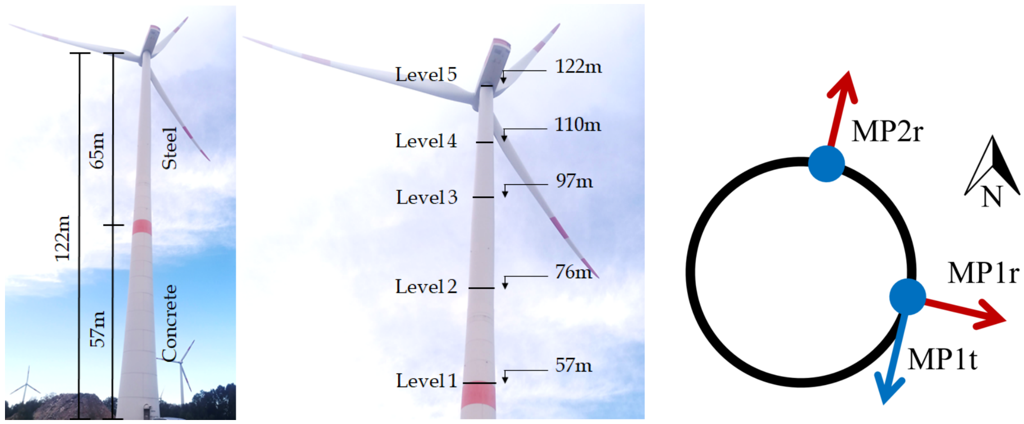

Figure 3: Sensor setup on the steel-concrete hybrid tower of a wind turbine. MP2 is aligned in 10° North and MP1 in 100° East.

which is advantageous in case of non-synchronous aggregated *Supervisory Control And Data Acquisition* (SCADA). The assignment of an identified mode to a bending mode pair is done when the S2MAC is greater than 0.8. Lower values of S2MAC are considered to be misidentifications.

However, for the distinction of the modes according to FA and SS within a bending mode pair, the nacelle position is required. This is achieved by classifying the mode whose directional angle γ is closest to the nacelle position as the FA-mode. The other mode is correspondingly assigned as the SS-mode.

3. Investigated hybrid concrete steel tower of a wind turbine

In this study, a hybrid concrete and steel tower of an 3.4 MW onshore wind turbine is investigated, which is shown in Figure 3. The first 57 m of the 122 m high tower consist of prestressed segmented concrete rings. The upper part is composed of steel tubes. The rated rotor speed of 14 rpm is reached at a wind speed of about 10 m/s. For the wind turbine under investigation, the main wind direction is West. This section first briefly describes the measurement setup. Subsequently, the dynamics of the tower is investigated on the basis of the first and fourth bending mode pairs.

3.1. Measurement setup

A measuring system is installed in an existing wind turbine. Because of limited accessibility, the five measuring levels coincide with the platforms of the towers. On each level, three *Integrated Electronics Piezo-Electric* (IEPE) accelerometers are installed. Two sensors measure in the radial direction of the tower, with a 90° angle to each other (MP1r and MP2r). An additional sensor of tangential direction is attached to one measuring point (MP1t) per measuring level, as shown in Figure 3. The calibrated IEPE sensors are combined with an IEPE supply with a cut-off frequency of 0.0106 Hz, enabling the measurement of acceleration signals without distortion down to 0.05 Hz [11]. The measurement data of all sensors are digitised synchronously with a 24 bit analogue to digital converter on Level 1 positioned and stored with a sampling rate of 500 Hz on a computer. The aim of this experimental setup is to investigate the dynamics of the hybrid tower in operation and to detect possible system changes over time. For the evaluation in this work, only the two acceleration sensors of MP1 from each measurement level are used. For a detailed study of the dynamics of the tower presented in the next section, measurement data sets from middle of October 2021 to end of September 2022 are used, assuming enough EOC variation during this period.

Mode pair	f_0 FA	f_0 SS	identification range	identification rate
1	0.309 Hz	0.297 Hz	0.24 Hz - 0.36 Hz	61.9%
2	1.445 Hz	1.475 Hz	1.25 Hz - 1.7 Hz	40.9%
3	3.144 Hz	3.036 Hz	2.8 Hz - 3.35 Hz	54.5%
4	3.602 Hz	3.788 Hz	3.35 Hz - 4.2 Hz	78.5%

Table 1: Median of the natural frequencies f_0, identification range and identification rate of the studied bending mode pairs for the selected EOC's in the period from middle of October 2021 to end of September 2022.

3.2. Dynamic of the tower

To use BAYOMA, the identification ranges must be defined a-priori, as described in Section 2.3. In the frequency range up to 5 Hz, four bending mode pairs occur. The identification ranges for these mode pairs are listed in Table 1. The mode shapes of these modes are shown in Figure 4. The bending modes

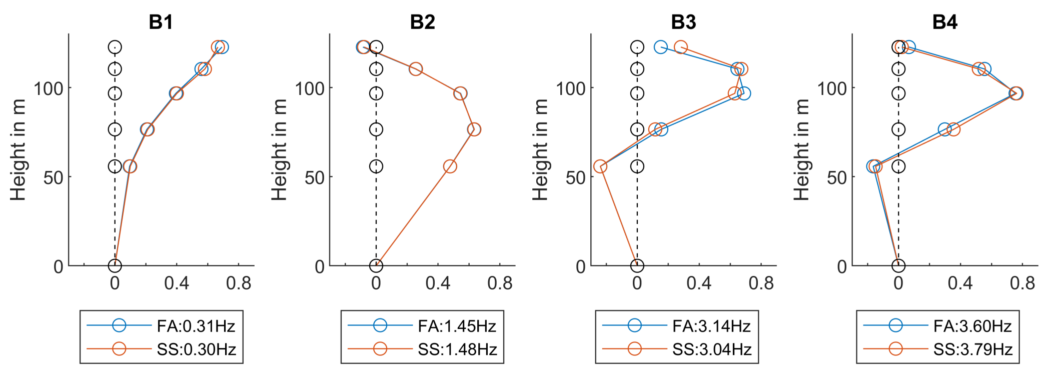

Figure 4: Mode shapes of the four bending mode pairs, identified under operation at a nacelle position of 270°, and rotated in the dominant direction for comparability.

are similar in FA and SS direction, respectively. The slight deviations may result from an asymmetric stiffness distribution around the circumference of the tower or the unevenly distributed head mass through the rotor and nacelle. Figure 5 shows the trend of the natural frequencies over time. As generally known, natural frequencies change over time due to EOCs. In addition, there

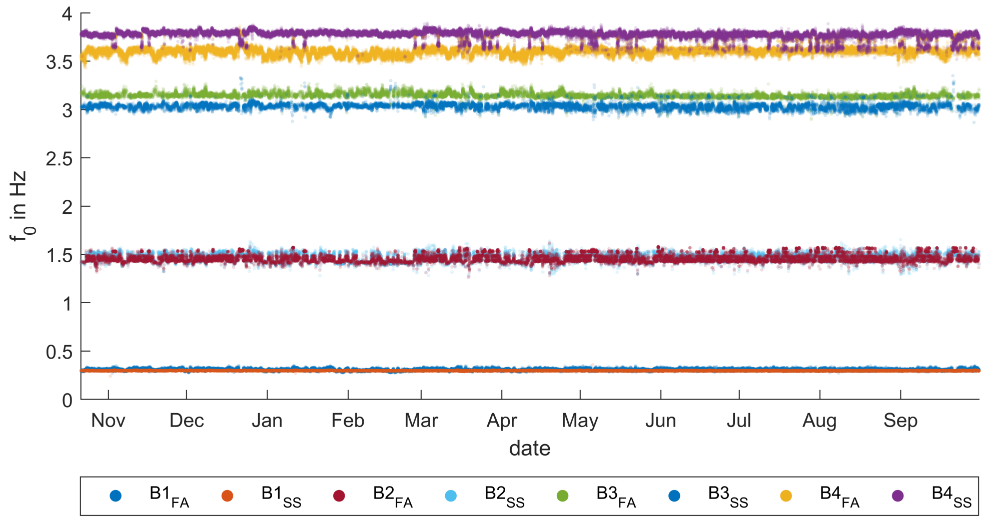

Figure 5: The natural frequencies of the four identified mode pairs plotted over time.

appear to be assignment issues, especially with the second and fourth mode pair. A better insight is provided by the Campbell diagram in Figure 6, which shows the natural frequencies as a function of rotor speed. The harmonic ex-

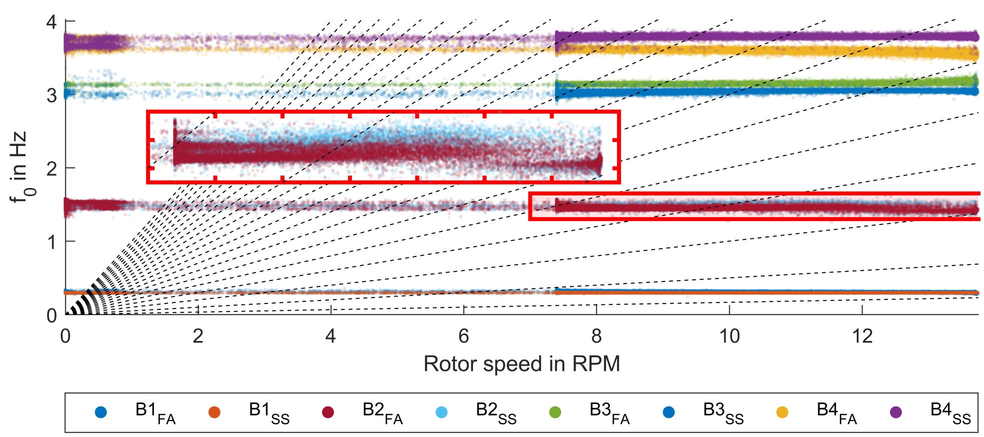

Figure 6: Campell diagram with the natural frequencies of the four lowest bending mode pairs.

citation has no relevant influence on the identification of the modal parameters as the dashed lines of the higher harmonics of the rotor speed do not correlate with the identified natural frequencies. In addition, the assignment problem of the fourth bending mode pair mainly occurs in standstill and start-up conditions. However, the second bending mode pair around 1.5 Hz scatters strongly and appears to have different states, depicted in the Campbell diagram. Hence, the assignment of the second bending mode pair does not work reliably. A cause for this behaviour could not be found, however, interactions with the rotor may be an explanation.

criterion	minimum	maximum	max standard deviation
power in kW	0	-	-
pitch angle in degree	-2	25	2.5
nacelle angle in degree	-	-	0.3

Table 2: Data selection criteria based on 10 minutes aggregated SCADA data.

In the following, this study focuses on the dynamics of the plant in operation. In order to exclude uncertainties due to transient time signals caused by the start-up and shut-down of the wind turbine as far as possible, only data sets are considered where the aggregated 10-minute SCADA data indicate constant operation. The selection criteria ensuring this are listed in Table 2. The medians of the identified natural frequencies, as well as the identification rate for the selected data are listed in Table 1. The reason for the relatively low identification rates is on the one hand that only completely identified bending mode pairs are used. In case of strongly unequal excitation of the pair, it may occur that only one mode is identified and the identification of the pair is thus incomplete. In addition, harmonic excitation and other transient effects can disturb the identification as in the case of the 2nd bending mode. In general, it is often

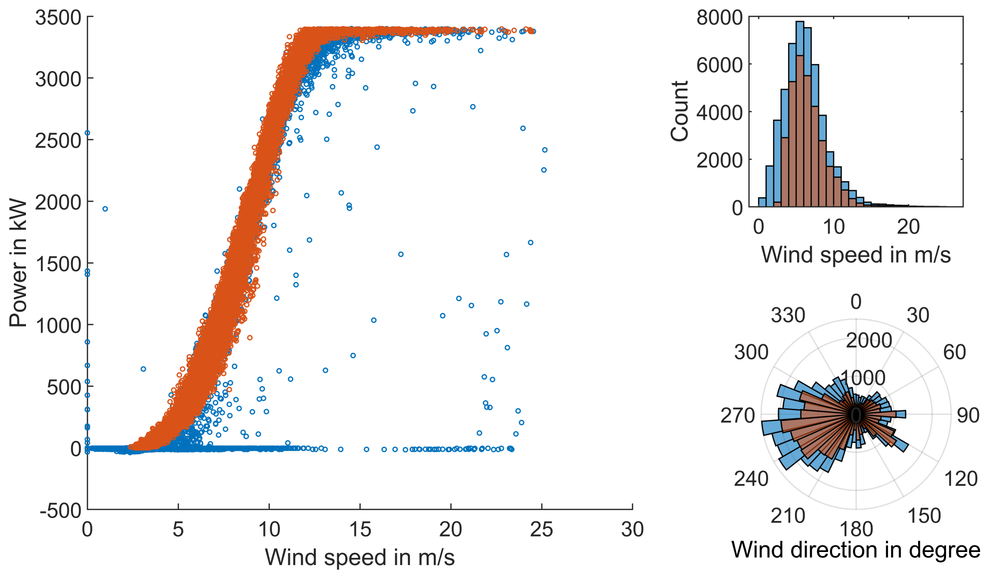

Figure 7: Power curve, wind speed and wind direction distribution of the investigated wind turbine, blue: all data, red: selected data (October 2021-September 2022).

the case that some modes are more difficult to identify when monitoring wind turbine towers [16], leading to lower identification rates. Figure 7 shows the power curve, the distribution of the wind speed and the wind direction of all data as well as the selected data during the almost 12 month period considered in this study. As stated before, only data sets belonging to operation conditions are used, and data points outside the expected power curve are not taken into account. Regarding the wind speeds, data sets below 2.7m/s are consistently omitted. Otherwise, the distributions of wind speeds and wind direction remain qualitatively the same. To exclude unconclusive identification results, identifications were not considered if the determined identification uncertainty of the natural frequency and damping was detected as an outlier using a Hampel filter [25] with a window length of 144, which corresponds to one measurement day.

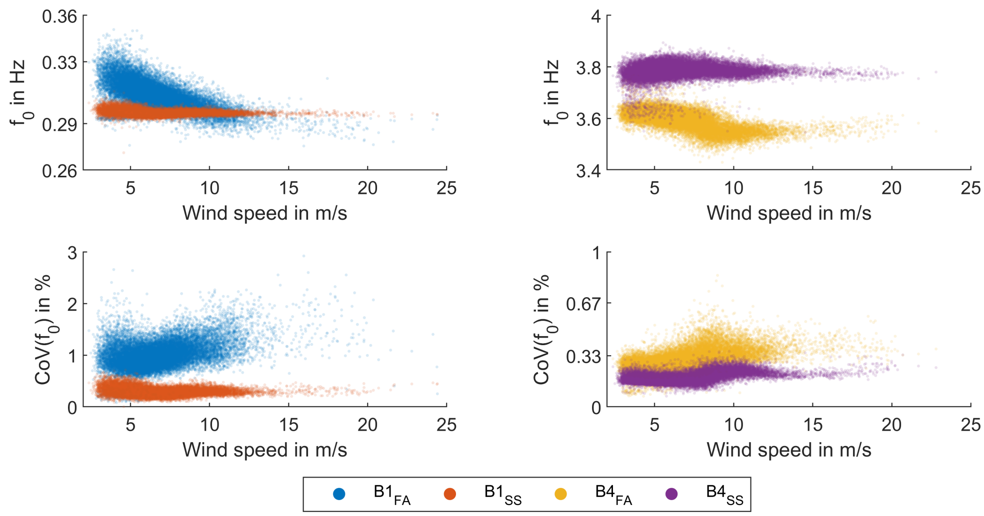

Figure 8: Top: Natural frequencies of the first and fourth bending mode pairs as a function of wind speed. Bottom: Coefficient of variation (CoV) in percent of the natural frequencies as a function of wind speed.

For further investigations, the first and fourth bending mode pairs are selected, as the first is the closest and the fourth is the best-separated mode pair. The top panel of Figure 8 shows the natural frequencies depending on the wind speed. The first bending mode in FA direction has a much stronger dependence on wind speed than the mode in SS direction. In addition, the observed scattering of the FA direction is significantly higher. Similar observations are made for the fourth bending mode pair, although the scattering is smaller. The identification uncertainty of the natural frequencies at the bottom of Figure 8 shows that the FA direction is identified with a higher uncertainty than the SS direction. The main reason for this difference is the aerodynamic damping [16], which leads to a significantly higher damping in the FA direction, as shown in Figure 9. A higher damping leads to higher identification uncertainties of the frequency. Since the damping of the first FA bending mode increases with

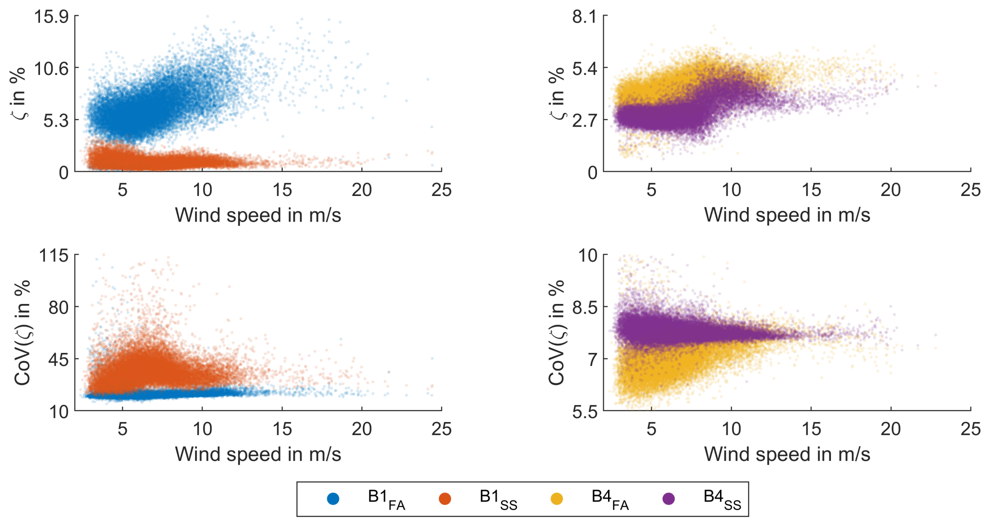

Figure 9: Top: Damping of the first and fourth bending mode pairs as a function of wind speed. Bottom: Coefficient of variation (CoV) in percent of the damping as a function of wind speed.

the wind speed, the identification uncertainty of the natural frequency also increases. For the fourth bending mode pair, the highest damping is determined between wind speeds of 4 and 12 m/s, so the corresponding natural frequencies are determined with the highest uncertainty in this range. In general, the identification of the damping is associated with significantly higher uncertainties than the identification of natural frequencies [20] and this can also be confirmed for the data sets used in this study. Regarding the uncertainties of the damping identification, in the lower panel of Figure 9 it is noticeable, that the damping identification of the SS modes is relatively more uncertain than the damping identification of the FA modes. However, the absolute uncertainty of the damping of the SS modes is still significantly lower than that of the FA modes. In addition, the damping of the fourth bending mode pair can be identified more reliably than the damping of the first mode pair. This is due to the length of the 10-minute data sets used. With an increasing number of vibration periods in the 10-minute interval, the damping identification becomes less uncertain. The uncertainty of the first bending modes in SS direction is remarkable, as the uncertainties in identification of the damping are more scattering at wind speeds below 10 m/s, as opposed to the trends observed for the other modes.

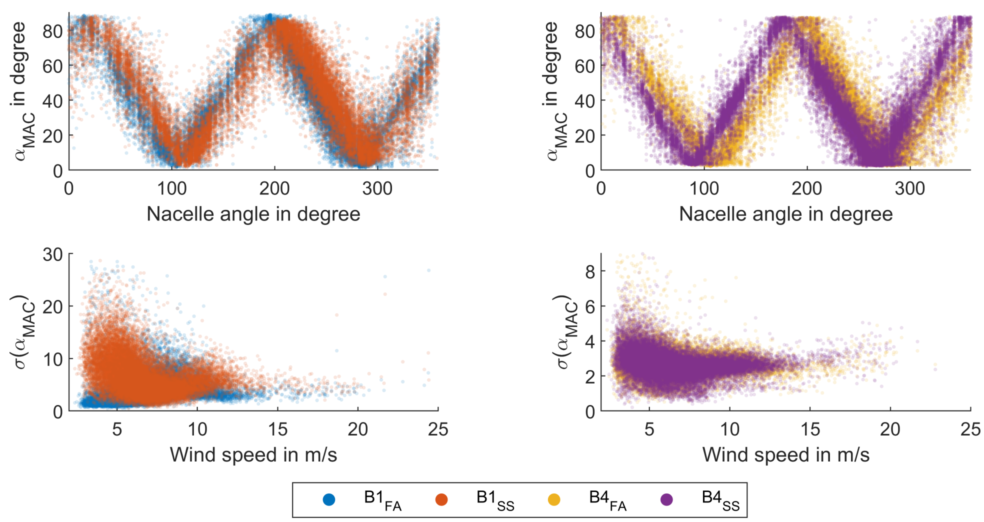

Figure 10: Top: α_{MAC} of the first and fourth bending mode pairs as a function of the nacelle angle. Bottom: Standard deviation of the α_{MAC} for the first and fourth bending mode pairs as a function of wind speed.

In the context of closely spaced modes, the mode shapes are of particular interest. The main uncertainty concerns the alignment of the mode shape in the mode subspace. In the case of wind turbine towers, the mode shape also changes due to the nacelle position. Therefore, in the top panels of Figure 10, the α_{MAC} for both pairs of modes is shown as a function of the nacelle position. The reference modes have been identified in the main wind direction at a nacelle position of 270°, so at that nacelle position, the α_{MAC} value is close to 0. There are few measurement data sets at nacelle positions below 100° and above 320°, which is due to the wind direction distribution. The deviation between the mode pairs depending on the nacelle position that can be observed in Figure 10 is due to the asymmetric stiffness distribution around the circumference, which may result from imperfections in the dry joints between the concrete segments or attachments. The uncertainty of the α_{MAC} is shown as a function of the wind speed. The fourth pair of bending modes is already well separated, so the uncertainty of the α_{MAC} is relatively small, which leads to a standard deviation of the direction angle of less than 5° for both bending modes. In the case of the first bending mode pair, the standard deviation of the α_{MAC} is very high at low wind speeds, especially for the SS mode.

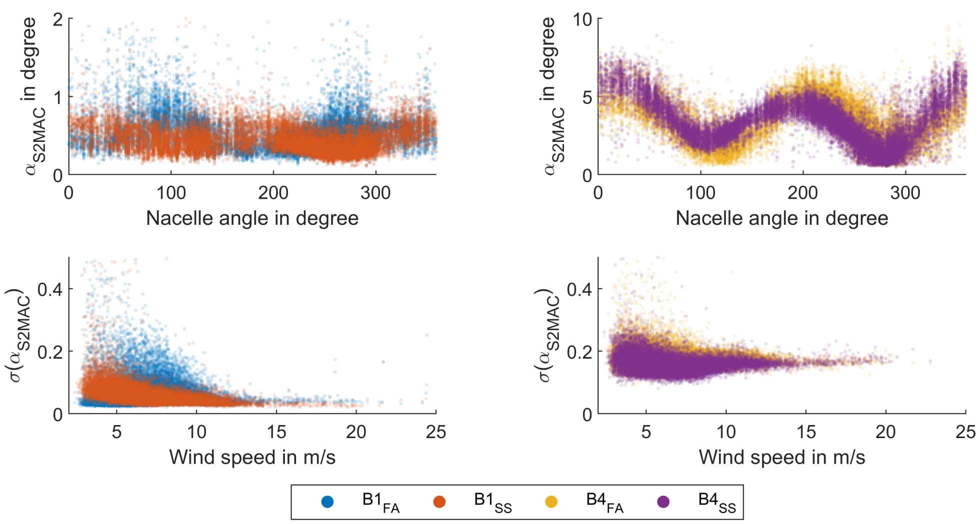

Figure 11: Top: α_{S2MAC} of the first and fourth bending mode pairs as a function of the nacelle angle. Bottom: Standard deviation of the α_{S2MAC} for the first and fourth bending mode pairs as a function of wind speed.

In contrast, the α_{S2MAC} depicted in Figure 11 changes less depending on the nacelle position. In particular, the first bending mode pair appears to have a relatively constant α_{S2MAC} regardless of the nacelle position. For the fourth bending mode pair, there is a clear dependence of the α_{S2MAC} on the nacelle position. This indicates that the mode subspace changes slightly as a function of nacelle position, which is presumably due to an asymmetric stiffness distribution over the circumference. The uncertainties of the α_{S2MAC} in Figure 11 are much lower than those of the α_{MAC} in Figure 10 for both bending mode pairs. This indicates that the α_{S2MAC} successfully eliminates the alignment uncertainty. Furthermore, the uncertainty of the α_{S2MAC} of the first bending mode pair is significantly lower than that of the fourth one. One reason could be a better signal to noise ratio, as has already been shown in [19]. In addition, the mode shape of the first bending mode pair has no nodal points at the sensor points considered, in contrast to the fourth bending mode pair, so that the measurement noise has a minor influence.

The direction angle γ expresses for symmetrical tower structures the alignment of the mode shape in the mode subspace [17] and is shown in Figure 12. The uncertainty of γ is higher the closer the modes are. As expected, the direction angle γ in the top of panel of Figure 12 depends linearly on the nacelle position. However, a larger scatter can be observed over the whole trend. This is due to the non-synchronous SCADA and the uncertainty of the direction angle shown in the bottom panel of Figure 12. The uncertainty is presented as a function of the wind speed. Considering this result, it is noticeable that

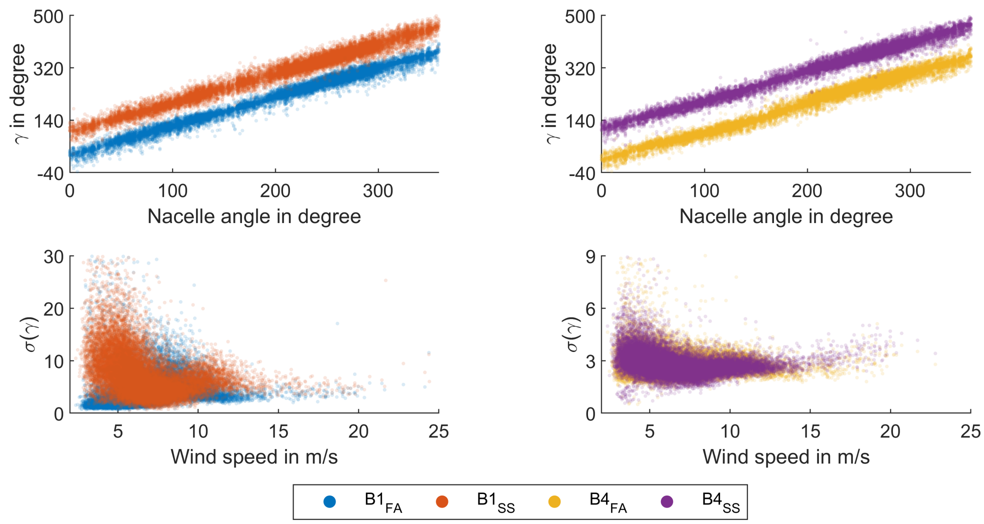

Figure 12: Top: Directional angle γ of the first and fourth bending mode pairs as a function of the nacelle angle. Bottom: Standard deviation of the directional angle γ as a function of wind speed.

the uncertainty of the direction angle is similar to the uncertainty of the α_{MAC} in Figure 10. This demonstrates clearly that the main uncertainty of the mode shapes of bending modes of wind turbine support structures originates from the alignment uncertainty within the mode subspace.

Throughout this investigation, it must be taken into account that the assumptions of BAYOMA, such as white noise as an excitation source and a linear time-invariant system, are violated. Therefore, the calculated uncertainties are indicative, but do not exactly correspond to the true uncertainties. However, for the practical application, it can be stated that BAYOMA can be used to obtain consistent dynamical identifications of the turbine structure of an onshore wind turbine.

Based on this investigation, it can be concluded that the α_{MAC} of the tower bending mode shapes with their high identification uncertainties independent of the nacelle position cannot serve as a reliable monitoring parameter. Instead, the identified mode shapes should be compared with a mode subspace using the α_{S2MAC}. This eliminates the high alignment uncertainty. As known from other studies [16], the more weakly damped SS natural frequencies can be identified more reliably than the FA natural frequencies. Nevertheless it is recommendable to also consider both natural frequencies as monitoring parameters, like [8, 16, 26].

4. Summary and Outlook

In this study, the applicability of BAYOMA to identify closely spaced bending modes from a tower of an onshore wind turbine in operation was investigated. The identification and the corresponding uncertainties provided plausible results despite the presence of harmonic excitation from the rotor. More strongly damped natural frequencies are much more uncertain to identify. Consequently, the less damped natural frequencies in SS direction can clearly be more reliably identified than the ones in FA direction. As typical for structures exhibiting closely spaced modes, the mode shapes can only be identified with high uncertainty, because the alignment of the mode in the mode subspace is very uncertain. Therefore, the α_{MAC} as well as the mode alignment angle are not suitable as reliable monitoring parameters. This does not apply to the α_{S2MAC}, which proved to be a reliable monitoring parameter, as already shown in previous studies for tower structures [19, 17].

Several future research approaches result from this study. In the onshore hybrid steel and concrete tower investigated, harmonic excitation did not have a significant impact, so that the identification of the modal parameters with BAYOMA worked well. For a more general statement it is thus necessary to investigate how harmonic excitation can affect the modal identification of wind turbine support structures constructed exclusively from steel, both onshore and offshore. The examination of the modal parameters clearly showed that they vary due to EOCs, so that the next step is to normalise the data for a reliable SHM-sheme. The uncertainties of the modal parameters indicate heteroscedasticity with respect to the EOC, i.e. a variability in dependence of the EOCs. Therefore, heteroscedastic Gaussian processes might be a good method for data normalisation to map this variability.

5. Acknowledgements

We greatly acknowledge the financial support of the German Research Foundation (CRC 1463, subproject C02), the Federal Ministry for Economic Affairs and Energy of Germany (research projects *Deutsche Forschungsplattform für Windenergie*, FKZ 0325936E and *PreciWind-Präzises Messsystem zur berührungslosen Erfassung und Analyse des dynamischen Strömungsverhaltens von WEA-Rotorblättern*, FKZ 03EE3013B) that enabled this work. In addition, we are grateful to the *Deutsche WindGuard GmbH*, as well as the *Bremer Institut für Messtechnik, Automatisierung und Qualitätswissenschaft* (BIMAQ) for their support during the measurement campaign.

6. Author contribution

Conceptualisation: C.J. Methodology: C.J. Formal analysis: C.J.; S.M. Investigation: C.J. Writing Original Draft: C.J. Visualisation: C.J.; L.L. Supervision: T.G.; R.R. Writing Review and Editing: S.M.; L.L.; B.H.; T.G.; R.R Resources: R.R. Funding acquisition: R.R. All authors approved the final submitted draft

References

[1] E. Commission, D.-G. for Environment, Guidance document on wind energy developments and EU nature legislation, Publications Office of the European Union, 2021. doi:doi/10.2779/095188.

[2] C. R. Farrar, K. Worden, An introduction to structural health monitoring, Philosophical transactions. Series A, Mathematical, physical, and engineering sciences 365 (1851) (2007) 303–315. doi:10.1098/rsta.2006.1928.

[3] K. Worden, L. A. Bull, P. Gardner, J. Gosliga, T. J. Rogers, E. J. Cross, E. Papatheou, W. Lin, N. Dervilis, A brief introduction to recent developments in population-based structural health monitoring, Frontiers in Built Environment 6 (2020). doi:10.3389/fbuil.2020.00146.

[4] C. R. Farrar, K. Worden, Structural health monitoring: a machine learning perspective, John Wiley & Sons, 2012.

[5] S.-K. Au, F.-L. Zhang, Y.-C. Ni, Bayesian operational modal analysis: Theory, computation, practice, Computers & Structures 126 (2013) 3–14. doi:10.1016/j.compstruc.2012.12.015.

[6] M. W. Häckell, R. Rolfes, Monitoring a 5MW offshore wind energy converter—Condition parameters and triangulation based extraction of modal parameters, Mechanical Systems and Signal Processing 40 (1) (2013) 322–343. doi:10.1016/j.ymssp.2013.04.004.

[7] C. Devriendt, F. Magalhães, W. Weijtjens, G. de Sitter, Á. Cunha, P. Guillaume, Structural health monitoring of offshore wind turbines using automated operational modal analysis, Structural Health Monitoring 13 (6) (2014) 644–659. doi:10.1177/1475921714556568.

[8] G. Oliveira, F. Magalhães, Á. Cunha, E. Caetano, Vibration-based damage detection in a wind turbine using 1 year of data, Structural Control and Health Monitoring 25 (11) (2018) e2238. doi:10.1002/stc.2238.

[9] C. Koukoura, A. Natarajan, A. Vesth, Identification of support structure damping of a full scale offshore wind turbine in normal operation, Renewable Energy 81 (8) (2015) 882–895. doi:10.1016/j.renene.2015.03.079.

[10] N. Penner, T. Grießmann, R. Rolfes, Monitoring of suction bucket jackets for offshore wind turbines: Dynamic load bearing behaviour and modelling, Marine Structures 72 (2020) 102745. doi:10.1016/j.marstruc.2020.102745.

[11] C. Jonscher, B. Hofmeister, T. Grießmann, R. Rolfes, Very low frequency IEPE accelerometer calibration and application to a wind energy structure, Wind Energy Science 7 (3) (2022) 1053–1067. doi:10.5194/wes-7-1053-2022.

[12] S.-K. Au, J. M. Brownjohn, B. Li, A. Raby, Understanding and managing identification uncertainty of close modes in operational modal analysis, Mechanical Systems and Signal Processing 147 (2021) 107018. doi:10.1016/j.ymssp.2020.107018.

[13] S. Bogoevska, M. Spiridonakos, E. Chatzi, E. Dumova-Jovanoska, R. Höffer, A data-driven diagnostic framework for wind turbine structures: A holistic approach, Sensors (Basel, Switzerland) 17 (4) (2017). doi:10.3390/s17040720.

[14] J. M. W. Brownjohn, A. Raby, S.-K. Au, Z. Zhu, X. Wang, A. Antonini, A. Pappas, D. D'Ayala, Bayesian operational modal analysis of offshore rock lighthouses: Close modes, alignment, symmetry and uncertainty, Mechanical Systems and Signal Processing 133 (2019) 106306. doi:10.1016/j.ymssp.2019.106306.

[15] W. Weijtjens, G. De Sitter, C. Devriendt, P. Guillaume, Automated operational modal analysis on an offshore wind turbine: Challenges, results and opportunities, in: 6th IOMAC: International Operational Modal Analysis Conference Proceedings, 2015, pp. 713–730.

[16] G. Oliveira, F. Magalhães, Á. Cunha, E. Caetano, Continuous dynamic monitoring of an onshore wind turbine, Engineering Structures 164 (2018) 22–39. doi:10.1016/j.engstruct.2018.02.030.

[17] C. Jonscher, L. Liesecke, N. Penner, B. Hofmeister, T. Grießmann, R. Rolfes, Influence of system changes on closely spaced modes of a large-scale concrete tower for the application to structural health monitoring, Journal of Civil Structural Health Monitoring 29 (8) (2023) 328. doi:10.1007/s13349-023-00693-6.

[18] W. D'Ambrogio, A. Fregolent, Higher-order mac for the correlation of close and multiple modes, Mechanical Systems and Signal Processing 17 (3) (2003) 599–610. doi:10.1006/mssp.2002.1468.

[19] C. Jonscher, B. Hofmeister, T. Grießmann, R. Rolfes, Influence of environmental conditions and damage on closely spaced modes, in: P. Rizzo, A. Milazzo (Eds.),

European Workshop on Structural Health Monitoring, Vol. 270 of Springer eBook Collection, Springer International Publishing and Imprint Springer, Cham, 2023, pp. 902–911. doi:10.1007/978-3-031-07322-9_91.

[20] S.-K. Au, Operational Modal Analysis: Modeling, Bayesian Inference, Uncertainty Laws, 1st Edition, Springer Singapore, Singapore, 2017. doi:10.1007/978-981-10-4118-1.

[21] K.-V. Yuen, L. S. Katafygiotis, Bayesian fast fourier transform approach for modal updating using ambient data, Advances in Structural Engineering 6 (2) (2003) 81–95. doi:10.1260/136943303769013183.

[22] R. J. Allemang, D. L. Brown, A correlation coefficient for modal vector analysis, Proceedings of the 1st International Modal Analysis Conference, Orlando: Union College Press 1 (1982) 110–116.

[23] E. Reynders, J. Houbrechts, G. de Roeck, Fully automated (operational) modal analysis, Mechanical Systems and Signal Processing 29 (5) (2012) 228–250. doi:10.1016/j.ymssp.2012.01.007.

[24] R. Brincker, P. Andersen, N.-J. Jacobsen, Automated frequency domain decomposition for operational modal analysis, Proceedings of the 25th SEM International Modal Analysis Conference, Orlando, Florida (2007).

[25] F. R. Hampel, The influence curve and its role in robust estimation, Journal of the american statistical association 69 (346) (1974) 383–393.

[26] W. Weijtjens, T. Verbelen, G. de Sitter, C. Devriendt, Foundation structural health

monitoring of an offshore wind turbine—a full-scale case study, Structural Health Monitoring 15 (4) (2016) 389–402. doi:10.1177/1475921715586624.